ARTICLE

Adhesion Forces Controlled by Chemical Self-Assembly and pH: Application to Robotic Microhandling

Jérôme Dejeu,* Michaël Gauthier, Patrick Rougeot, and Wilfrid Boireau

FEMTO-ST Institute, UMR CNRS 6174, UFC/ENSMM/UTBM, 24 rue Alain Savary, 25000 Besançon, France

ABSTRACT Robotic microhandling is a promising way to assemble microcomponents in order to manufacture a new generation of hybrid microelectromechanical systems. However, at the scale of several micrometers, the adhesion phenomenon highly perturbs the micro-object release and positioning. This phenomenon is directly linked to both the object and the gripper surface chemical composition. We propose to control the adhesion by using a chemical self-assembled monolayer on both surfaces. Different types of chemical functionalization have been tested, and this paper focuses on the presentation of aminosilane-grafted 3-(ethoxydimethylsilyl)propylamine and (3-aminopropyl)triethoxysilane. We show that the liquid pH can be used to modify the adhesion and to switch from an attractive behavior to a repulsive behavior. The pH control can thus be used to increase the adhesion during handling and cancel the adhesion during release. Experiments have shown that the pH control is able to control the release of a micro-object. This paper shows the relevance of a new type of reliable submerged robotic microhandling principle, which is based on adjustment of the chemical properties of the liquid.

KEYWORDS: microhandling • surface functionalization • aminosilane • adhesion • pull-off forces

INTRODUCTION

Manufactured products are getting smaller and smaller and are integrating more and more functionalities in small volumes. Several application fields are involved such as telephony, bioengineering, telecommunications, or, more generally speaking, the microelectromechanical systems (MEMSs). The assembly of these microproducts is a great challenge because of the microscopic size of the components (1). In fact, the major difficulty of microassembly comes from the particularity of the micro-object behavior, which depends on surface forces (2−4). The magnitude of the physical effects is drastically modified with a change in the scale from macroscopic (1 mm, for example) to microscopic (1 μm, for example), in which the lengths are divided by 10^3, the weights are divided by 10^9, and the surface forces (e.g., the van der Waals force) are divided only by 10^6. The effect of gravity thus decreases more rapidly than the effect of surface forces during miniaturization. So, on the microscale, the surface forces are predominant compared to the weight and the objects tend to stick the microgrippers. The manipulation of a micro-object requires handling, positioning, and releasing it without disturbances of the surface forces such as electrostatic forces, van der Waals forces, or capillary forces. The release is the most critical phase, which is usually hindered by adhesion.

Several methods have been proposed in the last 10 years to improve micromanipulation (5, 6). The first approach consists of using noncontact manipulation like laser trapping (7) or dielectrophoresis (8). These manipulation methods are not disturbed by adhesion. However, in an applicative context, micromanipulation has to be able to induce a large force (e.g., several μN) without displacement in order to assemble objects (e.g., insertion). In noncontact manipulation, the blocking force, which represents the maximal force applied on an object without displacement, stays low, which is a major drawback in the application field of microassembly. The second approach deals with contact manipulation, where the adhesion is reduced or directly used for manipulation. The reduction of the adhesion can be achieved, for example, by raising the roughness of the end effectors (9, 10). Adhesion can be directly used to perform manipulation tasks. In this case, a one-fingered gripper is sufficient to handle objects, but release remains difficult (11). In fact, new release methods are required such as inertial (12) or dielectrophoresis release (13). The major advantage of contact handling consists of the fact that the blocking force is usually high. The current microhandling methods are able to improve micromanipulation, but the object behavior is always disturbed by the adhesion and the reliability is still low (10, 14). The knowledge of adhesion forces is thus essential to enable the advent of reliable micromanipulation techniques. Current approaches are based on experimental measurements performed with atomic force microscopes (15−18), interferometric surface force apparatuses (19, 20), capacitive force sensors (21), nanoindentation testers (22, 23), tangential streaming potentials (24), or a measurement platform utilizing the contact mechanics theory of Johnson, Kendall, and Roberts (25). The adhesion force measurement is influenced by several parameters such as the preload force (26, 27), humidity (28), temperature (29), pressure (30),

* To whom correspondence should be addressed. E-mail: jerome.dejeu@univ-fcomte.fr.

Received for review May 20, 2009 and accepted August 18, 2009

DOI: 10.1021/am900343w

Published on Web 09/04/2009

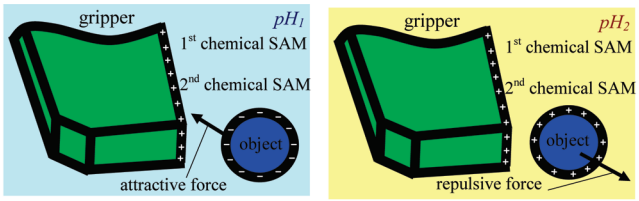

(a) handling in pH_1 where charges in SAM induces attractive force (b) release in pH_2 where charges in SAM induces repulsive force

FIGURE 1. Principle of robotic microhandling controlled by a chemical SAM.

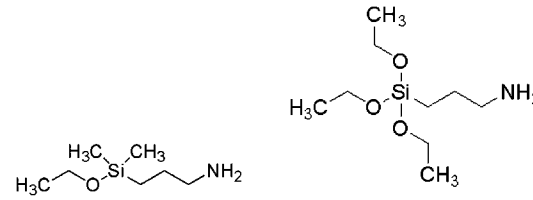

(a) APDMES (b) APTES

FIGURE 2. Molecules used for the silica functionalization.

roughness (31), and properties of the liquid medium (pH (32, 33) and ionic strength 32, 34).

We propose a new contact handling system that chemically controls the surface forces between the object and the gripper (15). We have already shown that the medium (air or liquid) can modify or cancel the adhesion force (15). The major objective is to control the adhesion force or to create a repulsive force to guarantee a reliable release. Now, the surface properties of a material can be controlled by surface functionalization in a liquid. The surface functionalization of the objects or of the grippers can be obtained by different methods. The two most important methods to form self-assembled monolayers (SAMs) are the polyelectrolyte physisorption (polyelectrolyte with positive or negative charges) (35) and the surface molecule grafting (covalent bond between the substrate and molecules) (36−38). This phenomenon is mainly due to two processes depending on the instrinsic atomic compositions of the substrates: oxidized substrates are useful for silane functionalization, whereas gold substrates are only reactive with thiol compounds. The difference in reactivity could be a real advantage in our approach because the use of silane (or thiol) molecules will allow a vectorization of the chemical processes. This could be a highly versatile tool to give specific properties to a precise part of the micro-objects especially in microassembly.

Grafting generates a covalent bond between the substrate and molecules. These molecules must contain silanol, thiol, azide, allyl, or vinyl groups (36, 37) in one extremity. These molecules have to be used in an organic solvent such as toluene, acetone, methanol, ethanol, etc. The silanol creates a Si−O−Si bond with the silica substrate (36), while allyl or vinyl generates a Si−O−C (or Si−C) bond (39) and the azide groups produce a Si−N bond (40). In this work, we choose silanization because the layer created did not exhibit any signature of degradation when stored in an airtight container for 18 months (41) and was stable up to a temperature near of 350 °C (42, 43), even when washed using 1 % detergent solution, hot tap water, or organic solvents and aqueous acid at room temperature (42). This silane layer was robust under the same daunting conditions that all existing semiconductor materials already endure such as thermal stability up to 350 °C and chemical stability under different etchants. So, the functionalized MEMS can be used in molecular and/or hybrid electronics. The charge density of the functionalized surfaces must depend on the pH in order to control the adhesion force in the liquid medium using the pH.

The microhandling principle is presented in Figure 1. The grasping can be done at pH_1, where the surface charges on the gripper and the object induce an attractive force. In order to release the object, the pH is modified to a second value, pH_2, where the object charge is changing. The electrostatic force becomes repulsive, and the object is released.

The microhandling method proposed is based on two chemical functions: amine and silica. On the one hand, the amine group is in the state NH_2 at basic pH and NH_3^+ at acidic pH. On the other hand, the silica surface charge in water is naturally negative except for very acidic pH, where the surface is weakly positive (44).

The objective of this article consists of showing the relevance of pH switching in controlling submerged microhandling. In the first section, we present the surface chemical functionalizations. In the second part, we analyze the interaction force measurement between two surfaces (functionalized and not functionalized or both functionnalized) in a liquid as a function of the pH in order to determine the charge density of the silane layer by a model of the surface charges. Finally, we deal with an experimental micromanipulation task between a glass sphere and a tipless atomic force microscope controlled by the pH solution.

EXPERIMENTAL DETAILS

Materials and Chemicals. Two silane functionalizations have been tested (see Figure 2): 3-(ethoxydimethylsilyl)propylamine (APDMES) and the silane (3-aminopropyl)triethoxysilane (APTES). Both chemical compounds (APTES and APDMES) used for surface functionalization are amine functions: NH_2, which can be protonated or ionized to NH_3^+ according to the pH. At acidic pH, the amine is totally ionized; then the ionization decreases and is null at basic pH (between pH 9 and 12). The silanes (APTES and APDMES), ethanol, sodium chloride (NaCl), sodium hydroxide (NaOH), and hydrochloric acid (HCl) were purchased from Sigma Aldrich.

The deposits were made on silicon substrates purchased from Tracit (45). Milli-Q water was obtained with Direct-Q3 of Millipore. The pH of the solution was measured with a pH-meter (Sartorius, PT-10) and an electrode (Sartorius, PY-P22) and adjusted with the addition of sodium hydroxide and hydrochloric acid just before measurement.

Surface Functionalizations. Before being functionalized, the wafers were cleaned by immersion in a piranha solution (2 parts H_2SO_4 and 1 part H_2O_2) for 25 min at 70 °C. **Caution!** *Piranha solution is highly corrosive and extremely reactive with organic substances. Gloves, goggles, laboratory coat, and face shields are needed for protection.* Then, the wafers were rinsed in Milli-Q water and ethanol before silanization (functionalization by silane: APDMES and APTES). Solutions were freshly prepared by direct dissolution in ethanol for silanes. The final silane concentration was 1 %. The surfaces were functionalized by immersion in solutions for one night at room temperature. In the silane solution, the molecules were grafted on the substrate

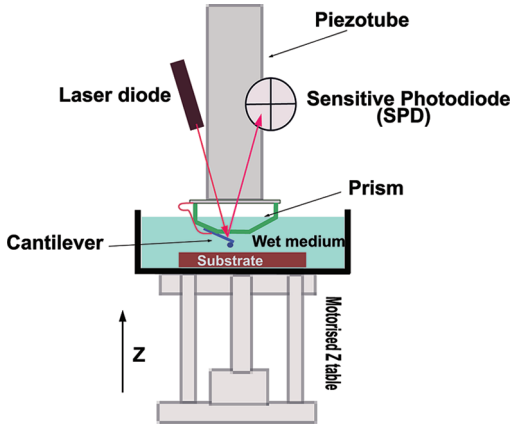

FIGURE 3. AFM-related setup used for force measurements.

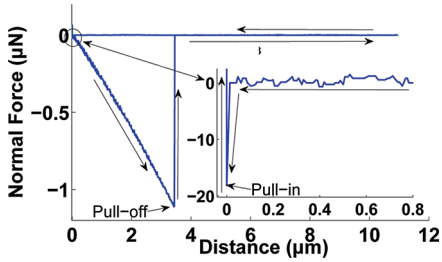

FIGURE 4. Force−distance curves obtained on functionalized APTES in an air medium (spring constant 0.3 N/m).

(covalent bond). The excess of ungrafted silanes was removed by ultrasonication for 2 min in ethanol. The mechanism of SAM formation during the silanization process is presented by Wasserman et al. (41)

Atomic Force Microscopy (AFM). In order to characterize the surface functionalization and to apply this functionalization to microhandling, a commercial atomic force microscope (standalone SMENA scanning probe microscope NT-MDT) was used. The experiment was done in the "nanorol platform", whose aim is to measure the micromanipulation nanoforce. The "nanorol platform" can be used by an external person. The availability and booking of the station is consultable via the Internet at http://nanorol.cnrs.fr/events.php.

AFM Force Measurement. Force measurements were performed in order to characterize the functionalizations. The force measurement performed on this atomic force microscope is based on the measurement of the AFM cantilever deformation with a laser deflection sensor (Figure 3). The silicon rectangular AFM cantilever, whose stiffness is 0.3 N/m, was fixed, and the substrate moved vertically. Because the applicative objective of this work is to improve the reliability of micro-object manipulation, interactions have been studied between a micrometric sphere and a plane. Measurements were, in fact, performed with a cantilever, where a borosilicate sphere (radius $r_2 = 5\,\mu$m) was glued onto the extremity and below this one (ref PT.BORO.SI.10' Novascan Technologies, Ames, IA). All measurements were done at a driving speed of 200 nm/s to avoid the influence of hydrodynamic drag forces (46). For each sample, nine measures were done at different points. The force standard deviation calculated for a number of nine pull-in and pull-off experiments was less than 10%.

Typical Distance−Force Curves. The first type of behavior is presented in Figure 4. In this case, an attractive force (pull-in force) is measured when the sphere is coming close to the substrate (near −20 nN; Figure 4). In Figure 4, we clearly measured a pull-off force, which represents the adhesion between the borosilicate sphere on the tip and the functionalized substrate. In this example, the pull-off force is reaching −1.1 μN. This behavior represents an attraction between the surfaces.

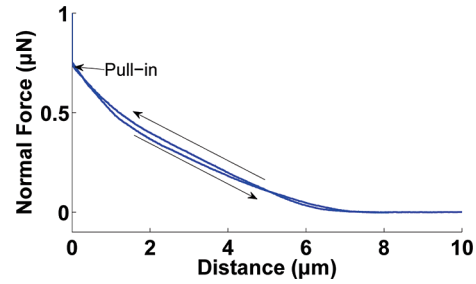

FIGURE 5. Force−distance curve obtained for the APDMES-functionalized substrate in a liquid medium (spring constant 0.3 N/m).

The second type of behavior is presented in Figure 5. In this case, there is repulsion between surfaces. We observe a repulsion (positive pull-in force near 0.75 μN) and no pull-off force between both surfaces. To summarize, an attractive interaction (respectively repulsive) is observed between the two surfaces when a pull-in force is negative (respectively positive), and the pull-off forces are always negative.

Micromanipulation. The aim of this force measurement is to find the conditions in a liquid medium where the properties of the grippers or the micro-object are switching in order to facilitate the grasping and release of the microcomponents. In order to verify the adhesion force measurement made by the AFM in the case of micromanipulation, we have done several experiments of pick and place, in different pH solutions. For this, we used a silicon tipless cantilever (Point Probe Technology) functionalized by APTES and glass spheres whose diameter was around 50 μm. The spring constant and resonance frequency at these tips were in the ranges of 0.02−0.77 N/m and 6−21 kHz, respectively.

RESULTS AND DISCUSSION

Influence of the pH on the Interaction. Experiments have been done in a liquid medium with the functionalized surface and a cantilever grafted with APTES or a nonfunctionalized cantilever. The pH of the solution varied by the addition of sodium hydroxide or hydrochloric acid. The surface stayed in the solution for 2 min before measurement, in order to equilibrate the system. Force measurement in a liquid has also been compared with measurement done in air.

Functionalized Surface. First, the measurements were done with a cantilever and a nonfunctionalized sphere. The measurements of the pull-in and pull-off forces are presented in Figure 6.

In this figure, we note that the pH influences significantly the forces between the cantilever and surface. At natural pH, an attractive pull-in is measured, near −60 nN, with an important pull-off of −350 nN (Figure 6a). When the pH increases, the pull-in force is inverted and becomes repulsive: 280 and 770 nN at pH 9 and 12 (parts b and c of Figure 6), respectively. Moreover, the adhesion forces disappear. The average values of the different measurements (pull-in and pull-off forces), at different pHs, are summarized in Table 1.

In this table, we observe that the phenomenon described above for APTES is the same as that for APDMES. In fact, at

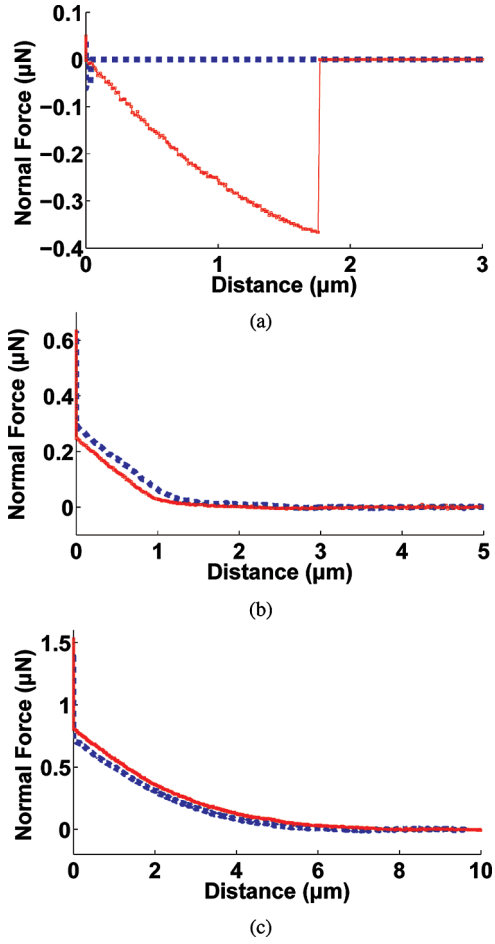

FIGURE 6. Force−distance curve for the APTES-functionalized substrate in a liquid medium at different pHs (spring constant 0.3 N/m): (a) pH natural (near pH 5.5); (b) pH 9; (c) pH 12. The dashed lines (blue) are the approach of the surface near the cantilever, and the full lines (red) are the retraction.

Table 1. Influence of the pH on the Pull-in and Pull-off Forces Obtained (Spring Constant 0.3 N/m) for APTES and APDMES Grafted on the Surface

	APTES		APDMES	
medium	pull-in (nN)	pull-off (nN)	pull-in (nN)	pull-off (nN)
pH 2	0	−176 ± 15	0	− 93 ± 14
natural pH	−59.5 ± 8	−387 ± 38	−29.8 ± 6	−353 ± 21
pH 9	282 ± 31	0	377 ± 49	0
pH 12	768 ± 63	0	1100 ± 130	0
air	−13.2 ± 1.5	−1150 ± 90	−4.97 ± 1	−769 ± 72

natural pH (near pH 5.5), the interaction is attractive with an important adhesion force and, at basic pH, above pH 9, the interaction is repulsive. At pH 2, we do not detect any pull-in force probably because the charge density on the silica cantilever was too low. In this table, we show that the forces measured with grafted APDMES are lower than those with APTES. We can explain this by the fact that the quantity of molecules grafted on the substrate is more important for APTES than for APDMES.

Because the charges on the surface of the silica cantilever are negative or null, the surface density σ of APTES and APDMES verifies that

$$\begin{array}{c}\text{for natural pH or pH 2, } \sigma \geq 0 \\ \text{for pH 9 or 12, } \sigma \leq 0\end{array} \quad (1)$$

In fact, at the pH of water (near pH 5.5−6), the positive charges induced by the functionalization are greater than the negative charges induced by the hydroxyl groups. At this pH value, the silica was weakly negative (47). At basic pH, the negative charges are predominant.

The inversion of the interaction forces during variation of the pH of the solution represents a great interest in micromanipulation. The control of the pH is, in fact, able to switch from an attractive behavior (grasping) to a repulsive behavior (release).

Functionalized Surface and Cantilever. Second, the cantilever was functionalized with the APTES silane and without a sonification step. Experiments similar to previous ones were performed in an aqueous solution of pH that varied between 2 and 12. The force−distance curves obtained with APDMES grafted on the substrate are presented in Figure 7.

Contrary to the previous case, the forces measured were always repulsive between the functionalized cantilever with APTES and the APDMES grafted on the surface. We did not detect any pull-off force. There was, in fact, no adhesion between both functionalized objects. A cantilever deformation was observed on an important distance (typically several micrometers) when the sphere is approaching from the surface. This distance increases with the value of the repulsion force. This large interaction distance typically is discussed in the following. The average values of the force measurements at different pH values are summarized in Table 2.

In this table, we note that the pH of the medium changes the value of the repulsive force between the cantilever and the surface but the behavior always remains repulsive. For acidic and natural pH, the repulsion can be explained by the positive charges of the aminosilane grafted on the surface. For basic pH, repulsion is induced by the negative charges of the silicon substrate down to the functionalization. Indeed, from pH 9, the positive charges of the aminosilane are not sufficient to totally screen the negative charges of the silicon. However, at pH 9, the charge screening induced by some NH_3^+ groups explains why the repulsions are lower with a functionalized cantilever (pH 9 in Table 2) than with a nonfunctionalized cantilever (pH 9 in Table 1). Moreover, at pH 12, the behaviors of the functionalized and nonfunctionalized surfaces are quite similar. In fact, the aminosilane has no positive charges left and the repulsion is only induced by the negative charges on silicon and borosilicate. However, the instability of the silane layer in basic solutions was already measured by Wasserman et al. (41). The monolayer immediately deteriorates upon exposure to an aqueous base, and a complete removal of the monolayer was observed within 60 min. The destruction of the monolayer in a highly basic solution (pH 12) is due to the hydrolysis of Si−O−Si bonds (41). The stability range depends on the silane molecules and on the substrate where it is grafted. In

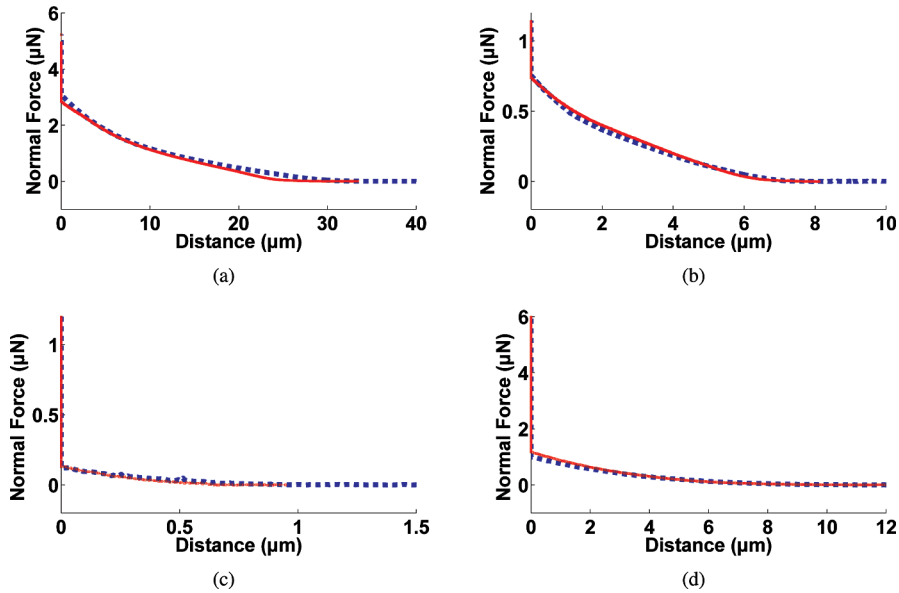

FIGURE 7. Force−distance curve for the APTES-functionalized substrate and cantilever in a liquid medium at different pH values obtained with a tip-functionalized APTES (spring constant 0.3 N/m): (a) pH 2; (b) pH natural (near pH 5.5); (c) pH 9; (d) pH 12. The dashed lines (blue) are the approach of the surface near the cantilever, and the full lines (red) are the retraction.

Table 2. Influence of the pH on the Pull-in and Pull-off Forces (nN) obtained with a Tip-Functionalized APTES (Spring Constant 0.3 N/m) for APTES and APDMES Grafted on the Surface

	APTES		APDMES	
medium	pull-in (nN)	pull-off (nN)	pull-in (nN)	pull-off (nN)
pH 2	3190 ± 247	0	3080 ± 223	0
natural pH	655 ± 50	0	735 ± 60	0
pH 9	150 ± 13	0	114 ± 15	0
pH 12	983 ± 62	0	989 ± 66	0
air	0	−91 ± 23	0	−136 ± 35

our case, the destruction of the silane layer is observed at pH 12 by the gradual decrease of the AFM laser-photodiode reading during force−distance measurement. Instead, we noticed no modification of the laser-photodiode value for pH 9, and subsequent measurements, repeated three times per day thereafter, were the same. So, the silane layer at pH 9 is stable. Also, when the cantilever was immerged in an acid solution at room temperature, the laser-photodiode value remained identical during the measurement, demonstrating the silane layer stability to acid pH. Lenfant (43) has already demonstrated the stability of the silane layer for a long period (up to a couple of days) at pH 1.

In micromanipulation, the repulsion between two objects is an interesting behavior in order to make easier the separation of two objects, whatever the pH of the solution. Indeed, the release of micro-objects will be easier if both the micro-object and gripper are functionalized with aminosilane, which induces the repulsive force.

Modeling of the Surface Charges. ***Multiscale Modeling.*** The range of the force measured is clearly greater than that of the current work done in electrical double-layer analysis, where the typical interaction distance is approximately several tens of nanometers (48−50). These studies present experiments and models of the coupling between the surface charges, the interaction distance, and the electrical surface potential for interaction distances lower than the that of the micrometer. In our case, the interaction lengths are greater than that of the micrometer and cannot be modeled by these approaches.

In the literature, some works deal with high long-range interaction on polymer surfaces (51, 52). The interaction distance has the same order of magnitude as that of our work, but the magnitude of forces was not measured. Explanations provided by the authors are based on thousands of layers of tightly bound water. We are proposing another explanation based on multiscale analysis:

In the nanoscale or in a chemical point of view, the distance between both surfaces greater than 1 μm could be considered as infinite. Each surface can be thus considered individually. Chemical interaction with the electrolyte induces an electrical charge density on the surface. We will show that the order of magnitude of this charge density is comparable to those predicted in the case of double-layer analysis.

In the microscale, both surfaces can be considered as uniformly charged surfaces whose charges are constant. The liquid medium can be modeled by a dielectric. Interaction forces can be deduced by Coulomb law between both surfaces. We will show that the interaction distance of several micrometers can be easily explained by Coulomb forces.

Model of the Coulomb Force. In order to determine an analytical relationship between the Coulomb force and the surface density on both surfaces, we assume that the surface is large enough to be considered as infinite compared to the sphere whose radius is $r_2 = 5\,\mu$m. The electric field E_1 induced by the surface charge density σ_1 of the substrate is uniform:

$$\vec{E_1} = \frac{\sigma_1}{2\varepsilon_3\varepsilon_0}\vec{n_1} \quad (2)$$

where ε_0 is the electric permittivity of the vacuum, ε_3 the relative permittivity of the medium (for water, $\varepsilon_3 = 80$), and $\vec{n_1}$ the unit vector perpendicular to the substrate. The repulsive Coulomb force applied by the gripper on the object whose charge is q_2 is thus

$$\vec{F}_{\text{pull-in}} = q_2\vec{E_1} = 2\pi {r_2}^2\frac{\sigma_1\sigma_2}{\varepsilon_3\varepsilon_0}\vec{n_1} \quad (3)$$

where σ_2 is the charge density on the sphere whose radius is r_2.

If both objects have the same surface density σ_1, the latter one can be deduced from the force measurement:

$$|\sigma_1| = \left(F_{\text{pull-in }1-1}\frac{\varepsilon_3\varepsilon_0}{2\pi {r_2}^2}\right)^{1/2} \quad (4)$$

The sign of σ_1 should be determined by considering the chemical functions (eq 1).

Moreover, in the case of an interaction between two different functionalized surfaces, the charge density σ_2 of the second surface is done by

$$\sigma_2 = \frac{F_{\text{pull-in }1-2}}{\sigma_1}\frac{\varepsilon_3\varepsilon_0}{2\pi {r_2}^2} \quad (5)$$

Identification of the Surface Charges. In the following, we assume that the surface densities on APTES grafted on borosilicate and on silicon are identical. Equation 4 has been used to determine the charge density of APTES (see Table 3). Equation 5 has been used to determine the electrical surface density of APDMES (see Table 3).

In this table, the sign of the charge density was determined according to eq 1. Buron et al. also found positive charge densities at natural pH (5.5) (53). The value of the charge density corresponds to a double-layer potential near 50 mV at pH 2. This potential value is widely found for surfaces deposited with polymers or silanes (54−56). In the case of a monolayer, it is generally found that the electrokinetic potential after adsorption has the same sign as the adsorbed polyelectrolyte, which means that there is an excess of the polymer charge density in comparison with the structural surface charge. Using the Gouy−Chapman relationship for diffuse layer charge density (57), the charge excess corresponding to a potential of around 50 mV can be calculated. Theoretical studies carried out by Cohen-Stuart et al. (56) and experimental illustrations (55) have shown that once the surface potential reaches a given value, an electrostatic repulsion is created in the interface that prevents additional molecules from reaching the substrate. In other words, polyelectrolyte adsorption is kinetically limited,

Table 3. Electrical Surface Density of the Functionalized Surface as a Function of the pH

	APTES	APDMES
pH	σ_1 (μC/cm^2)	σ_2 (μC/cm^2)
pH 2	+0.38	+0.36
natural pH	+0.17	+0.19
pH 9	−0.08	−0.06
pH 12	−0.21	−0.21

with a threshold for surface saturation when the ζ potential reaches about ±40 mV. This all applies well to the present measurements.

Interaction Distance Modeling. This section shows that Coulomb law between two surfaces whose surface charges are constant is able to induce high long-range interactions. A finite-element model of the Coulomb force between a finite surface and a sphere with an identical surface charge σ_1 (see Table 3) has been simulated with the software COMSOL Multiphysics 3.5. Comparative results between experiments and simulated forces are presented in Figure 8. It clearly shows that the model using Coulomb forces between two charged surfaces is able to explain both the high long range of the interaction and the level of force.

Application of Functionalized Surfaces in Micromanipulation. The behavior described in Table 1 shows a transition between attraction in natural pH and repulsion in pH 9. This switching behavior can be used to control the grasping and release of a micro-object manipulated with a microgripper. Two scenarios can be presented (see Figure 9). In the first case, grasping and release occur in two different media in order to guarantee adhesion during the grasping and repulsion during the release. In the second case, the pH of the medium has to be changed during manipulation. A microfluidic system could be built to induce laminar flow of an acidic or basic solution sequentially in the manipulation range. The laminar flow should be able to switch the pH rapidly without disturbing the position of the object on the substrate.

This microhandling method has been first tested on the AFM. Figure 10 shows the first experiments made with the AFM with a tipless cantilever functionalized with APTES and a free functionalization glass sphere. At natural pH, a glass sphere, whose diameter is around 50 μm, is "grasped" with the tipless cantilever (Figure 10a). For this, the cantilever was

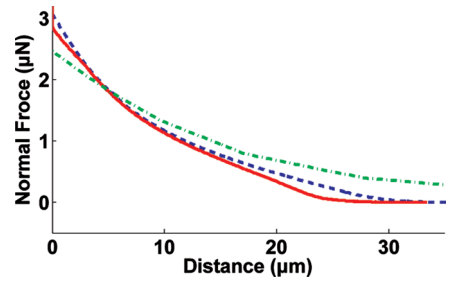

FIGURE 8. Experimental and simulated force−distance curve for the APTES-functionalized substrate and cantilever at pH 2. The dashed line (blue) is the experimental approach of the surface, the full line (red) is the experimental retraction, and the dash-dotted line (green) is the simulated Coulomb force.

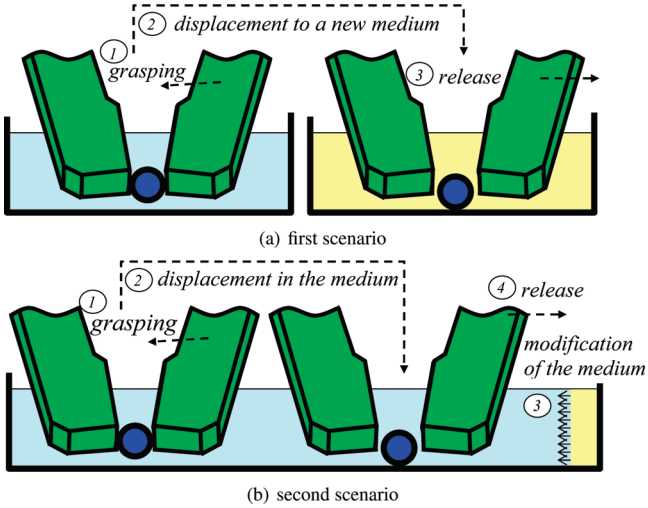

FIGURE 9. Scenarios of robotic microhandling coupling with chemical functionalization.

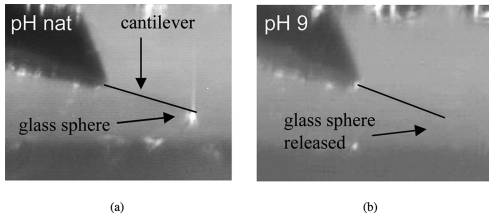

FIGURE 10. Grasping at natural pH (a) and release at pH 9 (b) of a sphere with a functionalized cantilever.

lowered down to the sphere and a force of 20 μN was applied. When the cantilever went up, the borosilicate sphere stayed attached to the cantilever thanks to the attractive force (natural pH) and the adhesion force, which are near 60 and 387 nN, respectively (Table 1). Afterward, the pH was increased by the addition of a NaOH solution. The behavior was inverted, and when the pH was near 9, the sphere was released (Figure 10b). Indeed, the attractive and adhesion forces disappeared and a repulsive force of 282 nN appeared between the cantilever and the sphere (Table 1).

CONCLUSIONS

In this paper, we have studied the interaction behavior between two functionalized surfaces and between functionalized and neutral surfaces. The experiments were done as a function of the pH of the liquid and compared with an air medium. The substrates were functionalized by two chemical compounds using silanization (grafted silane molecules). This technique was used because of the important stabilities of the silane layer such as thermal stability up to 350 °C and chemical stability under different etchants. We have shown that the functionalization and the pH of the medium could highly change the adhesion properties. The microassembly could be facilitated by a judicious choice of the media and of the functionalization of both grippers and micro-objects. We have shown that the pH can be used to control the release of a nonfunctionalized object during micromanipulation. Furthermore, the use of functionalized grippers and objects enables one to simply cancel adhesion on micro-objects. Because adhesion is the current highest disturbance in micromanipulation, functionalization is a promising way to improve micro-object manipulation in the future. This paper consists of a proof of concept of a new promising micromanipulation method. The complete characterization of this method based on repeatability measurements as well as reliability determination has to be performed. Future works will also focus on the implementation of this method, which is able to cancel adhesion perturbations on two-fingered microgrippers. The large blocking force required in microassembly will thus be possible.

Acknowledgment. This work was supported by the EU under HYDROMEL Contract NMP2-CT-2006-026622 (Hybrid ultra precision manufacturing process based on positional- and self-assembly for complex microproducts) and by the French National Agency (ANR) under NANOROL Contract ANR-07-ROBO-0003 (Nanoanalyse for micromanipulate). We also acknowledge the support of David Rostoucher and Alex Ivan for their English correction.

REFERENCES AND NOTES

(1) Tamadazte, B.; Dembélé, S.; Le Fort-Piat, N. *Sens. Transducers J.* **2009**, *5*, 37–52.
(2) Lambert, P. Capillary Forces. *Micro-assembly*; Springer: Amsterdam, The Netherlands, 2008.
(3) Gauthier, M.; Régnier, S.; Rougeot, P.; Chaillet, N. *J. Micromech.* **2006**, *3*, 389–413.
(4) Zhou, Q.; Chang, B.; Koivo, H. N. Ambient environment effects in micro/nanohandling. *Proceedings of the International Workshop on Microfactories*, Shangai, China, Oct 15−17, 2004; IOP Publishing Ltd.: Bristol, U.K., 2004; pp 146−151.
(5) Sariola, V.; Zhou, Q.; Koivo, H. N. *J. Micro−Nano Mech.* **2008**, *4*, 5–16.
(6) Lambert, P. *J. Micromech. Microeng.* **2006**, *16*, 1267–1276.
(7) Dholakia, K.; Reece, P.; Gu, M. *Chem. Soc. Rev.* **2008**, *37*, 42–55.
(8) Hunt, T. P.; Westervelt, R. M. *Biomed. Microdevices* **2006**, *8*, 227–230.
(9) Arai, F.; Andou, D.; Nonoda, Y.; Fukuda, T.; Iwata, H.; Itoigawa, K. *IEEE/ASME Trans. Mech.* **1998**, *3*, 17–23.
(10) Hériban, D.; Gauthier, M. Robotic Micro-assembly of Microparts Using a Piezogripper. *Proceedings of the 2008 IEEE/RSJ International Conference on Intelligent RObots and Systems*, IEEE: Nice, France, Sept 22−26, 2008; 2008; pp 4042−4047.
(11) Lambert, P.; Régnier, S. *Int. J. Micromech.* **2006**, *3*, 123–157.
(12) Driesen, W.; Varidel, T.; Régnier, S.; Breguet, J. *J. Micromech. Microeng.* **2005**, *15*, 259–267.
(13) Gauthier, M.; Gibeau, E.; Hériban, D. Submerged Robotic Micromanipulation and Dielectrophoretic Micro-object Release. *Proceedings of the IEEE ICARCV 2006 Conference*, IEEE: Singapore, Dec 5−8, 2006; 2006.
(14) Dafflon, M.; Lorent, B.; Clavel, R. A micromanipulation setup for comparative tests of microgrippers. *International Symposium on Experimental Robotics*, Rio de janeiro, Brazil, July 6−10, 2006; 2006. CD-ROM; available on-line on EPEL website.
(15) Dejeu, J.; Rougeot, P.; Gauthier, M.; Boireau, W. *Micro Nano Lett.* **2009**, *4*, 74–79.
(16) Wang, T.; Canetta, E.; Weerakkody, T. G.; Keddie, J. L. *ACS Appl. Mater. Interfaces* **2009**, *1*, 631–639.
(17) Gong, H.; Garcia-Turiel, J.; Vasilev, K.; Vinogradova, O. I. *Langmuir* **2005**, *21*, 7545–7550.
(18) Delettre, A.; Gauthier, M.; Rougeot, P.; Régnier, S. *Appl. Surf. Sci.* **2009**, submitted for publication.
(19) Blomberg, E.; Poptoshev, E.; Claesson, P. M.; Caruso, F. *Langmuir* **2004**, *20*, 5432–5438.
(20) Charrault, E.; Gauthier, C.; Marie, P.; Schirrer, R. *Langmuir* **2009**, *25*, 5847–5854.
(21) Rabenorosoa, K.; Clevy, C.; Lutz, P.; Gauthier, M.; Rougeot, P. *Micro Nano Lett.* **2009**, submitted for publication.
(22) Vajpayee, S.; Hui, C.-Y.; Jagota, A. *Langmuir* **2008**, *24*, 9401–9409.

(23) Murphy, M. P.; Kim, S.; Sitti, M. *ACS Appl. Mater. Interfaces* **2009**, *1*, 849–855.
(24) Dejeu, J.; Lakard, B.; Fievet, P.; Lakard, S. *J. Colloid Interface Sci.* **2009**, in press.
(25) Nolte, A. J.; Chung, J. Y.; Walker, M. L.; Stafford, C. M. *ACS Appl. Mater. Interfaces* **2009**, *1*, 373–380.
(26) Yeo, C.; Lee, S.; Polycarpou, A. *Rev. Sci. Instrum.* **2008**, *79*, 015111-1–015111-8.
(27) Tormoen, G.; Drelich, J. *J. Adhesion Sci. Technol.* **2005**, *19*, 181–198.
(28) Cleaver, J.; Tyrrell, J. *Kona* **2004**, *22*, 9–22.
(29) Tambe, N.; Bhushan, B. *Nanotechnology* **2004**, *15*, 1561–1570.
(30) Heim, L.; Blum, J. *Phys. Rev. Lett.* **1999**, *83*, 3328–3331.
(31) Haiat, G.; Barthel, E. *Langmuir* **2007**, *23*, 11643–11650.
(32) Xu, L.; Vadillo-Rodriguez, V.; Logan, B. *Langmuir* **2005**, *21*, 7491–7500.
(33) Sigmund, W.; Sindel, J.; Aldinger, F. *Prog. Colloid Polym. Sci.* **1997**, *105*, 23–26.
(34) Bowen, W.; Doneva, T.; Austin, J.; Stoton, G. *Colloids Surf., A* **2002**, *201*, 73–83.
(35) Decher, G. J. S. *Sequential Assembly of Nanocomposite Materials*; Wiley-VCH: New York, 2003.
(36) Demirel, G.; Caglayan, M. O.; Garipcan, B.; Piskin, E. *Surf. Sci.* **2008**, *602*, 952–959.
(37) Maas, J.; Stuart, M. C.; Sieval, A.; Zuilhof, H.; Sudhölterb, E. *Thin Solid Films* **2003**, *426*, 135–139.
(38) Mangeat, T.; Berthier, A.; Elie-Caille, C.; Perrin, M.; Boireau, W.; Pieralli, C.; Wacogne, B. *Laser Phys.* **2009**, *19*, 1–7.
(39) Moreau, O.; Portella, C.; Massicot, F.; Herry, J.; Riquet, A. *Surf. Coat. Technol.* **2007**, *201*, 5994–6004.
(40) Wang, J.; Guo, D.-J.; Xia, B.; Chao, J.; Xiao, S.-J. *Colloids Surf., A* **2007**, *305*, 66–75.
(41) Wasserman, S.; Tao, Y.-T.; Whitesides, G. *Langmuir* **1989**, *5*, 1074–1087.
(42) Ulman, A. *An Introduction to Ultrathin Organic Films From Langmuir—Blogett to Self-Assembly*; Academic Press: New York, 1991.
(43) Lenfant, S. Ph.D. Thesis, University of Science and Technology, Lille, France, 2001.
(44) Dove, P. M.; Craven, C. M. *Geochim. Cosmochim. Acta* **2005**, *69*, 4963U4970.
(45) Agnus, J.; Hériban, D.; Gauthier, M.; Pétrini, V. *Precision Eng.* **2009**, in press (corrected proof available online Feb 28, 2009).
(46) Vinogradova, O. I.; Yakubov, G. E. *Langmuir* **2003**, *19*, 1227–1234.
(47) Foissy, A.; Persello, J. *The Surface Properties of Silicas*; John Wiley & Sons: New York, 1998.
(48) Adamson, A. W.; Gast, A. P. *Physical Chemistry of Surface*, 6th ed.; Wiley-Interscience Publication: New York, 2002.
(49) Briscoea, W. H.; Attardb, P. *J. Chem. Phys.* **2002**, *11*, 5452–5464.
(50) Attard, P. *Adv. Chem. Phys.* **1996**, *92*, 1–159.
(51) Zheng, J.; Pollack, G. H. Solute Exclusion and Potential Distribution Near Hydrophilic Surfaces. In *Water and the Cell*; Pollack, G. H., Cameron, I. L., Wheatley, D. N., Eds.; Springer: Amsterdam, The Netherlands, 2006; Chapter 8, pp 165—174.
(52) Zheng, J.-M.; Pollack, G. H. *Phys. Rev. E: Stat., Nonlinear, Soft Matter Phys.* **2003**, *68*, 031408-1–031408-7.
(53) Buron, C.; Filiatre, C.; Membrey, F.; Bainier, C.; Charraut, D.; Foissy, A. *Colloids Surf., A* **2007**, *305*, 105–111.
(54) Dejeu, J.; Buisson, L.; Cyrille Roidor, M. C. G.; Membrey, F.; Charraut, D.; Foissy, A. *Colloids Surf., A* **2006**, *288*, 26.
(55) Geffroy, C.; Labeau, M.; Wong, K.; Cabane, B.; Stuart, M. C. *Colloids Surf., A* **2000**, *172*, 47.
(56) Cohen-Stuart, M.; Hoogendam, C.; de Keizer, A. *J. Phys.: Condens. Matter* **1997**, *9*, 7767.
(57) Hunter, R. *Introduction to Modern Colloid Science*; Oxford University Press: Oxford, U.K., 1993.

AM900343W